LuXSensing Beacon: Batteryless IoT Sensor, Design Methodology, and Field Test for Sustainable Greenhouse Monitoring

Kang Eun Jeon, Tsz Ngai Lin, James She, Simon Wong, Rajesh Govindan, Tareq Al-Ansari, and Bo Wang, *Senior Member, IEEE*

***Abstract*—Greenhouse farming is a trending practice to secure food production in desert environments. Such a practice often requires sensing systems to monitor the greenhouse microclimate. However, traditional monitoring systems are often limited by their feature size, energy consumption, and maintenance cost. To address these issues, this article introduces a luXSensing beacon—an energy harvesting sensing device empowered with Bluetooth communication technology to perform continuous environmental sensing. To enable long-lasting or even batteryless operation of the sensing device, we propose a novel and generic design methodology to suggest minimum energy harvesting hardware requirements, namely the photovoltaic panel's area and supercapacitor's size for energy storage. In addition, a lifetime model is also proposed to calculate the extended lifetime of a hybrid energy harvesting device if it is equipped with a backup battery. Based on the proposed methodology, a prototype system is developed, deployed, and tested in a desert greenhouse. The luXSensing beacon demonstrated its capability of monitoring air temperature and illuminance continuously in a 24/7 manner. The comparative compactness and low-energy consumption of the system are advantageous not only to its deployment in greenhouses but also to the reduction of energy budget and the maintenance cost of greenhouse farming.**

***Index Terms*—Bluetooth low energy (BLE) beacon, greenhouse monitoring, Internet of Things (IoT) sensor, LuXSensing beacon, self-powered wireless sensing.**

I. Introduction

FARMING is a great challenge in desert climates due to various limiting factors, such as low precipitation and high evaporation rates. Greenhouse technology, which helps overcome climatic constraints by providing crops with a suitable growing environment, is adopted in many arid countries for food production (e.g., Qatar and UAE). Sensing systems are often installed in greenhouses to monitor microclimatic conditions, such as air temperature, solar radiation, and CO_2 level in real time. The collected data allow a smarter control of various environmental parameters in greenhouses to maintain optimal crop growth conditions [1], [2].

However, most of the existing greenhouse sensing systems come with the limitations of bulkiness and high energy consumption, which leads to a high life cycle cost (LCC) of greenhouse operation, including the capital, operational, energy, maintenance, and repair costs [3]. In particular, traditional battery-powered sensors installed in greenhouses require batteries for power supply, thereby incurring significant energy and maintenance costs [4]. To reduce LCC, only a limited number of sensors can be installed in a greenhouse. However, environmental conditions in greenhouses can differ within a small spatial scale (e.g., within a few meters), and the absence of a wider grid of sensors to produce microclimate map results in a narrow scope of spatial observation of the target parameters, rendering the optimization of greenhouse control difficult to achieve. This inevitably results in reduced food production and water and energy wastage [5], [6], [7].

The increasing availability of Bluetooth Low Energy (BLE)-based wireless sensing technologies on the market reflects the tremendous demand for a monitoring system that can be made cost-effective, energy-efficient, and capable of providing real-time supervision. For example, BeaconTrax [8] provides a BLE module (Trax10127T) [9] for temperature and humidity sensing along with cloud service, which has a 2.8-year life span. However, the fact that the module is powered by batteries still renders its capability to be deployed on a large scale. To address issues such as the high cost of battery replacement, data discontinuity during system maintenance, and disposal problems, going batteryless is a more promising way for the next-generation wireless sensing system.

Everactive [10] is one such provider of a batteryless and always-on Internet of Things (IoT) sensing device (Eversensor). However, Eversensor [11] is too bulky to be deployed in existing plastic or glass greenhouses without renovation. In

Manuscript received 15 February 2023; revised 12 May 2023; accepted 12 June 2023. Date of publication 2 August 2023; date of current version 19 December 2023. This article was recommended by Associate Editor Andrea Boni. *(Corresponding authors: James She; Bo Wang.)*

Kang Eun Jeon is with the Department of Electronic and Computer Engineering, Hong Kong University of Science and Technology, Hong Kong, and also with the Convergence Research Institute, Sungkyunkwan University, Suwon 16419, South Korea (e-mail: kejeon@ust.hk).

Tsz Ngai Lin was with the College of Science and Engineering, Hamad Bin Khalifa University, Doha 34110, Qatar. He is now with Qualcomm, CB4 0WZ Cambridge, U.K. (e-mail: tngai@hbku.edu.qa).

James She, Rajesh Govindan, Tareq Al-Ansari, and Bo Wang are with the College of Science and Engineering, Hamad Bin Khalifa University, Doha 34110, Qatar (e-mail: pshe@hbku.edu.qa; rgovindan@hbku.edu.qa; talansari@hbku.edu.qa; bwang@hbku.edu.qa).

Simon Wong is with the Department of Electronic and Computer Engineering, Hong Kong University of Science and Technology, Hong Kong (e-mail: tywongbf@connect.ust.hk).

Digital Object Identifier 10.1109/TAFE.2023.3295383

TABLE I
COMPARISON OF DIFFERENT ENERGY HARVESTING BLE BEACON DEVICES

	GCell Solar iBeacon [15]	**Cypress SolarBeacon [13]**	**TIDA Indoor Light Harvesting Beacon [16]**	**HKUST SolarBeacon X1**
			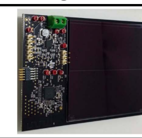	
Size	$123 \times 61 \times 25$ mm^3	25 mm diameter × 5.5 mm	86.36×60.96 mm^2	$12 \times 28 \times 36$ mm^3
BLE Chipset	TI CC2541	Cypress CYBLE-022001-00	TI CC2541	nRF51822
Sensing Capabilities	Illuminance	Temperature + humidity	None	None
Rechargeable Energy Storage	Capacitor (2 mF)	Supercapacitor (0.2 F)	Supercapacitor (8 mF)	Li-ion battery (17 mAh)
Backup Energy Storage	AA batteries	Not supported	Not supported	Not supported
Min. Required Illuminance (lm)	N/A	100 lx	250 lx	250 lx
Min. Advertising Interval @ lm	N/A	30-45 s	1 s	1 s
Limitations	Cannot operate without disposable battery	Very long sensing and advertising interval	Small rechargeable energy storage	Difficult to recharge in indoor environment

comparison, Infineon [12] developed a compact batteryless solar BLE sensor (CYALKIT-E02) [13] to transmit ambient temperature and humidity data using the BLE broadcasting mode. Being the smallest solar-powered BLE sensor currently available on the market, its 0.2-F on-chip supercapacitor allows a 30-h continuous operation without ambient light. However, the tight power budget of the sensor limits its sampling rate, which is as long as 5 min/sample when the supercapacitor is being charged. In desert greenhouse farming, this is a significant drawback as the desert environment exhibits rapid changes. The lack of real-time data may result in over-/undershoot in the microclimate control. A sensing system with a small sensing interval is more favorable.To address these issues, this article presents a lightweight, cost-effective, and self-powered luXSensing beacon sensing system for greenhouse applications. Two environmental parameters, air temperature and illuminance, are chosen among others in this study as proof of concept since they are the key factors affecting crop growth [3], [14]. With a dimension of $66.4\times56.9\times18.5$ mm^3 and a sensing interval of one sample per minute, the proposed system is capable of large-scale deployment in greenhouses to collect comprehensive spatial data in a 24/7 manner, which could enable more precise monitoring and microclimate control. The contributions of our article can be summarized as follows:

1) developing a novel data-driven design methodology that integrated the use of a supercapacitor as rechargeable storage to maximize device lifetime/sustainability while minimizing form factor;
2) constructing a luXSensing beacon to collect illuminance and temperature data, optimizing it based on illuminance data collected from a desert greenhouse in Qatar;
3) conducting real-world field tests using luXSensing beacons to monitor illuminance and temperature data at a desert greenhouse.

The rest of this article is organized as follows. Section II provides a brief discussion of IoT technologies for greenhouse applications. Section III presents the proposed luXSensing beacon. Section IV presents the design methodology with special consideration on its power budget. Section V describes the sensor deployment and the measurement results obtained from our field test. Finally, Section VI concludes this article.

II. BACKGROUNDS AND RELATED WORKS

In this section, we present the background knowledge on energy harvesting devices and greenhouse applications empowered by IoT technologies. We first present existing energy harvesting BLE beacon designs and their shortcomings. Then, we review various enabling IoT and communication technologies with real-life application examples.

A. Energy Harvesting BLE Beacons

To enable self-sustainable and maintenance-free IoT applications, several solar-powered BLE beacons from the industries have been proposed, as shown in Table I. GCell Solar iBeacon [15] and TIDA Indoor Light Harvest [16] have large form factors, which make them unsuitable for deployment in greenhouses. On the other hand, Cypress SolarBeacon [13] has slow energy harvesting speeds to support the energy consumption of the sensors. Most BLE beacons rely on disposable coin cell batteries as their main power source. The lifetime and form factor of the beacon may vary depending on the cell used. A review of battery-powered BLE beacons can be found in [31]. Shih et al. [17] used a combination of RF and light harvesting to operate a BLE beacon system with a long advertising interval of 45 s. HKUST SolarBeacon X1, the first prototype developed by the authors, also has similar drawbacks. The device was designed to operate in low-light environments; however, it was found that the rechargeable Li-ion battery could not be recharged with such a small current source. Existing devices have insufficient energy harvesting capabilities to support the required advertising interval of 1000 ms, and lack of energy storage capacity restricts them to short life spans if there is no ambient light energy. This makes direct conversion of existing battery-powered infrastructure to a batteryless one unreliable, considering that most interactive applications require an advertising interval below 1000 ms. In response to this, numerous attempts have been made to realize batteryless IoT infrastructure. Mekikis et al. [18] analyze connectivity in a batteryless sensor network under different routing schemes. Huang et al. [19] investigate deployment schemes for IoT applications and propose a general framework, optimization model, and low-power-consuming optimization algorithm to support green IoT.

B. IoT Technologies for Greenhouses

The utilization of IoT in smart farming has boomed in recent years [20], [21]. Mobile monitoring/manipulating systems have been regularly adopted in precision agriculture applications such as spatial imaging, pest detection, and on-field sensing for crop and soil monitoring (i.e., soil moisture, conductivity, salinity, etc.) [22], [23], [24]. Since mobility and precision are the main concerns for precision agriculture applications, satellite navigation systems for positioning and laser/infrared tracking for localization are very popular among mobile systems. Meanwhile, perceptual layers of IoT devices need to be integrated into the mobile system when environmental information from different spaces needs to be collected.

Previously, some IoT platforms used predefined values or hard-coded models to handle specific tasks in the greenhouse. Now, these tasks can be managed individually and simultaneously to boost crop productivity by taking advantage of the real-time measurement of IoT devices and the adaptive control from cloud computing services. The following are three of the many developed schemes that reach their individual goal using IoT sensing devices. FarmBeats, an IoT platform developed by Microsoft Research for data-driven agriculture, uses drone videos and sensor data to generate a precision map for the farm and monitor solar radiation with the weather-aware IoT base station. With FarmBeats gateway connected to IoT base station and Azure cloud via Wi-Fi, a duty cycling approach is also deployed for the sensor module to achieve energy neutrality and data continuity [25]. AgriSens, a dynamic irrigation scheduling system for water management, monitors the water level using IoT devices and performs irrigation based on the crop's life cycle phases. With the help of ZigBee, the sensor node, actuators, and weather station can be linked to the farmer's side for monitoring and remote control [26]. Greenhouse models as a service (GMaaS), a cloud-based service model that can forecast the following 48-h climate change, crop production, and irrigation values inside a greenhouse, is proposed to build a platform for crop production. A single-page application, iVeg, is also developed as a graphical front end for the user to call the GMaaS directly instead of requesting it via HTTP protocol [28]. Yıldırım et al. [29] employed RFID temperature sensors along with wireless power transfer techniques to enable sustainable and reliable greenhouse monitoring. The deployment cost, especially the reader cost, hinders its applicability in standard greenhouses.

The fundamental IoT revolution in the greenhouse depends on communication technologies that can fulfill energy efficiency, broad coverage, and scalability. Different communication technologies distinguish the speed of the range, power consumption, and operating (uploading and downloading) [30]. Table II summarizes the distinct choices of protocols. First, good connectivity/bandwidth can ensure the correctness and timeliness of the data. Second, encrypted/secured information can prevent hacking and exclusive the data to specific users. Last but not least, minimal sufficient communication can avoid battery depletion and allow the usage of self-sufficient power sources. While having the lowest power consumption among other IoT technologies, BLE-empowered infrastructure can support multiple applications simultaneously. Namely, BLE infrastructure can serve as both perceptual and also localization layers. Moreover, the infrastructure's robustness and energy efficiency eliminate the hassle of deploying and managing power-hungry heterogeneous infrastructure, leading to accelerated deployment/development of BLE-beacon-based infrastructure for smart farming applications.

To this end, we propose a novel design methodology for energy harvesting BLE sensor devices, which determines the solar panel area and supercapacitor size to maximize the chance of self-sustainable operation while minimizing the cost and form factor. The proposed methodology is employed to develop luXSensing beacons which are later deployed for a field test at a desert greenhouse in Qatar. The field-test results demonstrate that the prototyped luXSensing beacon can collect various sensor data reliably in a 24/7 self-sustainable manner.

III. Proposed Greenhouse Sensing System

An overview of the proposed luXSensing beacon is shown in Fig. 1. The device is equipped with two sensors for measuring air temperature and illuminance. The system also contains a small solar panel for energy harvesting, a supercapacitor for energy storage, and a Bluetooth module for communication. A simplified schematic of the device is shown in Fig. 2, which highlights the sensing module, luXSensing beacon, and communication module. The details of the design of this device are as follows.

A. Air Temperature and Illuminance Sensing

The sensing module consists of a low-dropout linear regulator (LDO) TPS782, a temperature sensor TMP36, a photoresistor (PR) CDS-55, and a bias resistor (R_b). The LDO regulates the output from the solar energy harvester, supplying a stable 3.3 V output to the temperature sensor and the PR. Note that the sensing module requires are dedicated voltage regulator as it requires stable 3.3 V for accurate and reliable sensing measurements, whereas the microcontroller unit (MCU) can accept a wide range of voltage from 1.8 to 3.6 V, thanks to its internal regulator. The temperature sensor has an accuracy of $\pm 1\,^\circ$C at $+25\,^\circ$C. The PR is able to respond to both indoor ($\sim$20 kΩ) and

TABLE II
COMPARISON OF DIFFERENT COMMUNICATION TECHNOLOGY FOR GREENHOUSE APPLICATION

Protocol	IEEE Standard	Range	Data rate	Power consumption	Applications
WiMAX	IEEE 802.16	$<$ 50 km	1 Gbit/s	High	Vast area coverage, UAVs communication
Wi-Fi	IEEE 802.11	20–150 m	9.6 Gbit/s	High	Portable devices, accessing cloud, sensor nodes and gateways communication
ZigBee	IEEE 802.15.4	10–100 m	250 kbit/s	Medium	Interconnection in mesh networking, localized communication,irrigation management
LoRa/LoRaWAN	IEEE 802.15.4g	2–5 km	0.3–50 kbit/s	Low	Long-range connectivity, low-rate application, water monitoring
Bluetooth	IEEE 802.15.1	10–50 m	2 Mbit/s	Low	Low-power, short-range communication, high volume data, large deployment coverage

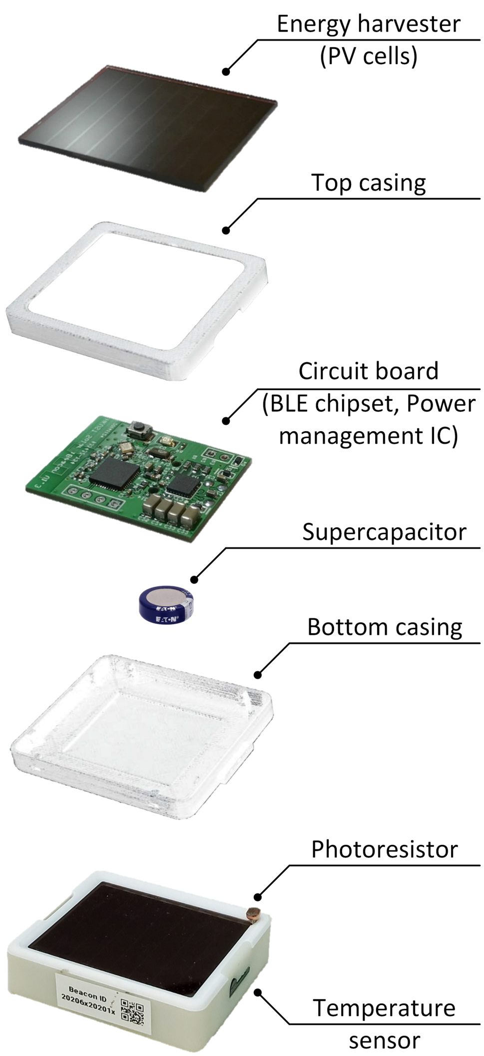

Fig. 1. Hardware components and packaging of the proposed sensing system for greenhouse application—the luXSensing beacon.

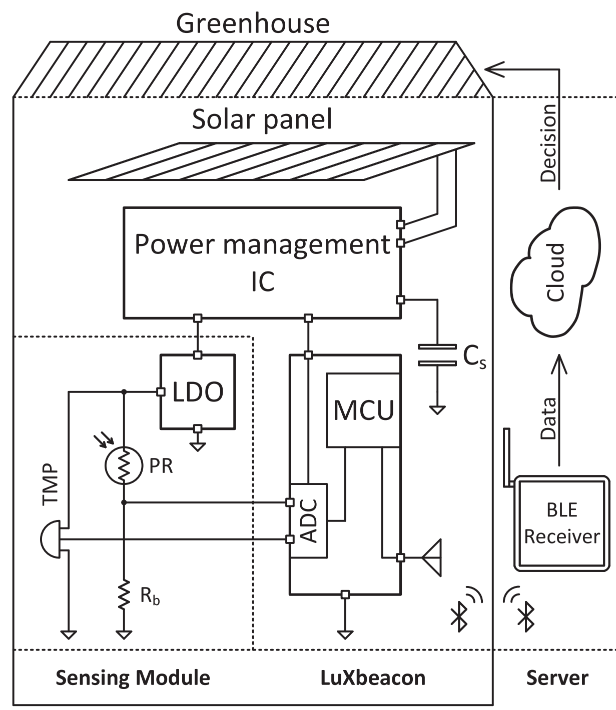

Fig. 2. Schematic of the proposed system with the integration of the sensing module (photoresistor and temperature sensor), luXSensing beacon, and communication module (BLE receiver, data collection, processing, and visualization in cloud).

outdoor ($\sim$100 Ω) light conditions. The voltage divider formed by the PR and a 497-Ω resistor R_b provides an output voltage that ranges between 15 mV (low illuminance end) and 3.29 V (high illuminance end). With a supply of 3.3 V, the total current consumption of the sensing module is less than 6.7 mA, which is equivalent to the usage of 4% energy storage per hour. The low power consumption of the sensing module relaxes the energy budget of the energy harvester, allowing the sensing module to operate 24 h continuously.

In this design, a PR is used for illuminance sensing instead of a photodiode based on the comparative advantage of the former reflected by experimental results, which are shown in Fig. 3. Although a photodiode offers better signal linearity, it is not applicable for wide-range sensing (10^0–10^5 lx) because of its large current consumption under direct sunlight (>200 mA at 10^5 lx). Such a large current consumption will drain the capacitor rapidly, causing the whole module to shut down within 1 h (estimated by discharging a 1.5-F capacitor with 200 mA). In contrast, the voltage divider formed by a PR limits the maximum current consumption and, in turn, attenuates the voltage change at high illuminance (e.g., lower sensing resolution is needed when illuminance is high). Overall speaking, a PR is a better candidate for illuminance sensing as it offers a good tradeoff

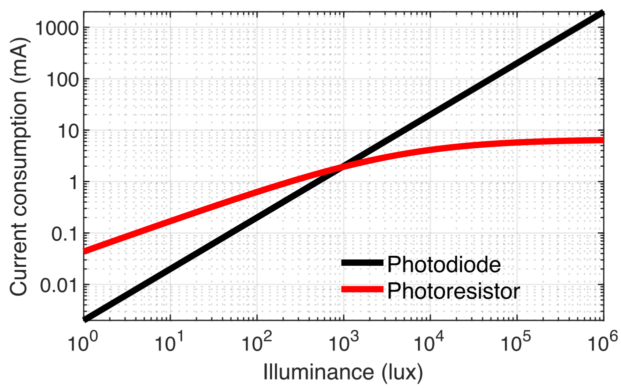

Fig. 3. Experimental results of the current consumption of photodiode and photoresistor versus illuminance in the range of 10^0–10^5 lx.

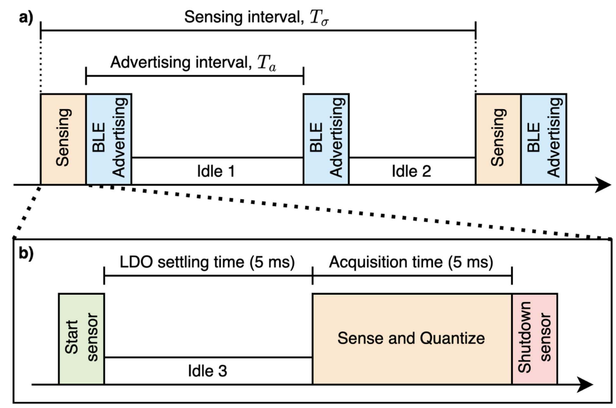

Fig. 4. (a) and (b) Timing diagram presenting the communication and sensing operation of a luXSensing beacon. Idle 1, 2, and 3 represent the idle state of the beacon but only with different duration.

between power consumption and linearity. The adopted PR is calibrated using the lux meter, and the percentage error of the current consumption is $\pm 2.2\%$ for >5000 lx.

B. Energy Harvesting and Communication

The second component of the proposed sensing system is a luXbeacon, which is used for sensor signal quantization and data transmission. LuXbeacon, the primary version of luXSensing beacon, first introduced in 2019 for location-based applications, is an energy harvesting BLE device that broadcasts short advertisement packets to its surrounding. BLE beacons are often employed in smart and interactive applications, such as localization and proximity detection [31]. Together with a sensing module, BLE devices are equipped with nRF52832 chipset, which supports Bluetooth 5 and is also backward compatible with previous versions, such as Bluetooth 4.2 and 4.1. The device can support an advertising interval ranging from 20 to 10 240 ms and transmission power from −20 to +4 dBm. This allows the luXSensing beacon to support a maximum broadcasting distance of up to 100 m. In this design, considering the requirements of the sensing application, the luXSensing beacon was configured with a less frequent advertising interval, T_a, of 1000 ms and transmission power of 0 dBm to support a maximum broadcasting range of up to 50 m, which meets the requirement of many modern greenhouses [32]. An overview of the BLE beacon's operation behavior is shown in Fig. 4(a). We can see that the BLE beacon spends most of its time in an idle state and only wakes up every T_a to conserve its energy. On the other hand, sensor measurements are taken every sensing interval, T_σ. It should be noticed that the sensing task happens right before the advertising task such that the latest sensing measurements are broadcasted. The selection of the advertisement configurations supports the required data advertisement to the nodes that report the data. Besides, short advertisement intervals lead to more energy consumed, e.g., the energy consumption will be almost doubled if the advertisement interval is half.

Furthermore, luXSensing beacon as a self-sustainable device addresses the issues of energy consumption and maintenance of sensing systems, which have been the bottleneck of large-scale deployment of sensor nodes in greenhouses [33]. It uses photovoltaic (PV) cells as the energy harvester to capture readily available light energy and employs a supercapacitor (C_s) for energy storage [34], thereby enabling long-lasting and batteryless operation of the device. The voltage generated by the PV cell ranges from 1.8 to 3.6 V, which matches the operating voltage of the BLE IC employed in our proposed design. Since the BLE IC is already equipped with efficient dc–dc switching and LDO regulators, we exploited the existing regulator rather than adding an external dedicated one so as to achieve reduced manufacturing cost and better efficiency. To cater to constrained environments where the harvestable ambient light energy is insufficient to support energy-neutral operation, the proposed luXSensing beacon design can be equipped with a backup energy storage or battery. That is, the luXSensing beacon can draw power from the backup battery when the supercapacitor is fully discharged or when it is not harvesting enough energy. With the advantage of reduced or even eliminated energy consumption, the use of a luXSensing beacon is conducive to the reduction in associated maintenance and repair costs. In addition, the small size of a luXSensing beacon facilitates its installation on various horizontal and vertical surfaces. By avoiding the hassle of bulky power supply, the deployment of luXSensing beacon in greenhouses is more convenient and scalable compared to its widely employed counterparts [20].

In this proposed sensing system, the luXSensing beacon consists of one power management IC (S6AE103A) and one BLE IC (nRF52832). The device can monitor the internal energy storage status and regularly transmit the energy information along with its unique identity via Bluetooth. The on-chip analog-to-digital converter (ADC) is used to quantize the sensor signal with 8-bit resolution, corresponding to 1.3 °C temperature sensing resolution and an average illuminance sensing resolution of 38 lx for <5000 lx and 1668 lx for >5000 lx. A voltage detection function is implemented in the device to prevent any sudden power-down caused by empty energy storage. After each power-ON operation (e.g., sensing request), the device checks the energy status, and the ADC only quantizes the sensor output when the threshold is reached.

A small sensing interval is desired in desert greenhouses where environmental conditions exhibit rapid changes. Considering the adverse impact that rapid environmental changes may have on plant growth [35], the sensing interval of this device is selected to be 1 min. Meanwhile, a shutdown capability is provided for the sensors to reduce the power supply drain. During the shutdown, the output of the sensors becomes high impedance such that the output potential is only determined by the external circuitry and the current draw is minimum. However, a start-up process is needed for the sensors to switch from shutdown to normal operation. During the start-up, data are not available, and this appears as a delay to the whole system. The longer the start-up process, the larger the delay added to the sensing system and as well as the amount of energy wasted. Thus, limited by the LDO settling time, the evaluation time is set to 10 ms (5 ms for the LDO start-up and settling, and 5 ms for ADC quantization as shown in Fig. 4), after which the power supply to the sensors is immediately cut off [36]. A timing diagram that details the sensor operation is shown in Fig. 4(b). We can see that the sensor is started and the device goes to an idle state to wait for the LDO to settle. Once the voltage of LDO can support reliable sensor measurement, the device acquires the sensor measurement through its ADC. After that, the sensor is shut down to minimize its energy consumption.

C. Data Collection and Processing

To record and analyze the collected data, a cloud server, the third component of the proposed system, is employed. The packet of the luXSensing beacon is structured as 29 bytes such that two sensor readings (8-bit each) can fit in. After collecting the packets, the BLE receiver groups all the packets and sends them to the cloud server for real-time processing. To reduce the required bandwidth, the grouped data are sent to the server every 5 min from the BLE receiver. Any outliers that may occur due to quantization errors on the ADC of the luXSensing beacon are filtered out. Moreover, the cloud server provides various postprocessing functions, such as moving average filter with configurable window size, and visualizations for easier data analysis and comparison. The sensed data can be used to optimize crop yield and/or reduce maintenance costs by controlling ventilation, humidity, and lighting inside the greenhouse. For example, based on the sensed illuminance, automated curtains can be controlled to precisely allow the optimal amount of sunlight to the crops. On the other hand, the temperature can be controlled energy efficiently through automated windows, finding the equilibrium with the temperature outside the greenhouse. In the future, additional sensors, such as humidity sensors, can be added to support other control mechanisms. The humidity sensor can help to control the amount of moisture delivered to the crops, thereby boosting the crop yield rate.

IV. Design Methodology for LuXSensing Beacon

To enable 24/7 operation, the energy budget of the luXSensing beacon has to be carefully modeled before prototyping and deployment. To achieve this, we propose a novel design methodology that optimizes energy harvesting hardware design,

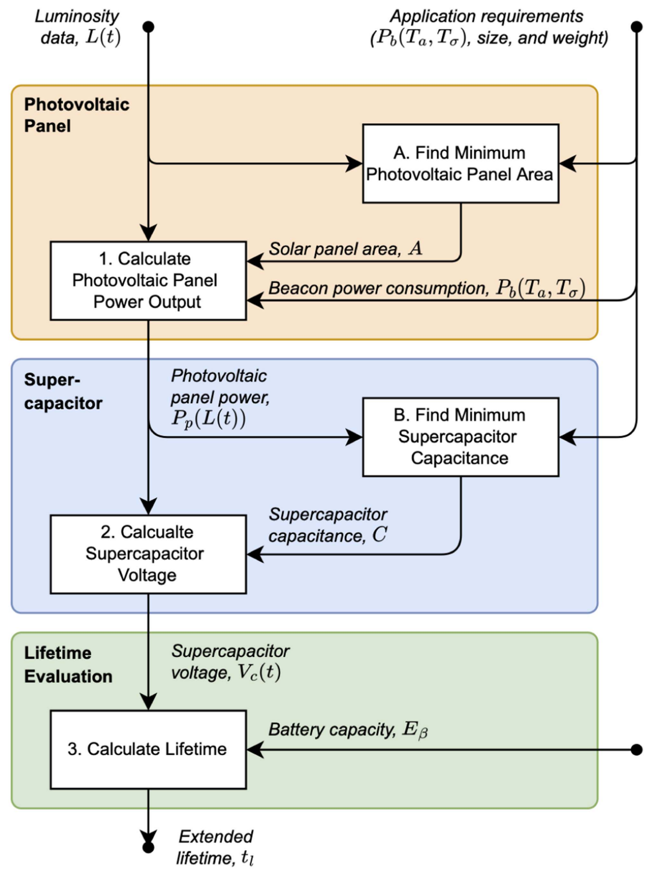

Fig. 5. Overview of the proposed design methodology.

namely PV panel area and supercapacitor capacitance, to enable long-lasting and even self-sustainable operation based on collected environmental sensor information, such as illuminance. Moreover, the methodology also enables accurate lifetime evaluation of an energy harvesting device equipped with a backup battery through the calculation of the supercapacitor's charging and discharging behavior.

The proposed design methodology is presented in Fig. 5. First, the minimum PV panel area to sustain the operation of a sensor device is calculated based on power requirements and the deployment environment's illuminance conditions. The calculated area is then utilized to generate the power output of the panel. The power output of the PV panel is combined with the power requirements of the sensor to calculate the net power consumption/harvested of the device. Second, the net power is used to calculate the minimum supercapacitor capacitance to guarantee reliable device operation in the absence of ambient light. The calculated capacitance is then utilized to calculate the charging and discharging behavior of the supercapacitor. Finally, the calculated behavior is used to calculate the portion of sensor operation time powered by a backup battery and evaluate the extended lifetime. The luXSensing beacon can support most types of coin cells, and we use CR2477 [38] in our experiments. The proposed design methodology may not necessarily achieve self-sustainable operation due to limited illuminance at the deployment environment, high power requirements, and weights,

TABLE III
COMPARISON OF SUPERCAPACITOR CAPACITANCE AND CORRESPONDING DIMENSIONS AND WEIGHTS

Capacitance (F)	**Length** (mm)	**Height** (mm)	**Weight** (g)
0.5	16.00	6.00	3.2
1.0	16.00	6.00	3.5
1.5	21.50	9.50	8.5
50	18.00	42.00	15.8

size, and cost limitations of PV panels and supercapacitors. Such tradeoff in capacitance and its physical specifications are detailed in Table III. However, given these restrictions, the proposed methodology aims to minimize the area of the PV panel and supercapacitor capacitance while maximizing the extended lifetime.

In order to design a long-lasting energy harvesting device, it is imperative to model the power consumption of a sensing beacon given some application requirements. The average power consumption of a sensing beacon, $P_b(T_a, T_\sigma) \in \mathbb{R}_{>0}$, is given by

$$P_b(T_\sigma, T_a) = \frac{E_\sigma}{T_\sigma} + \frac{E_a}{T_a} + P_i \tag{1}$$

where $\mathbb{R}_{>0}$ is a set of positive real numbers excluding 0 defined as $\mathbb{R}_{>0} = \{x \in \mathbb{R} | x > 0\}$; $T_\sigma \in \mathbb{R}_{>0}$ is the time interval between two sensing samples, which is bounded by $T_\sigma^{\min} \leq T_\sigma \leq T_\sigma^{\max}$, representing the hardware limitation and application requirements for the sensing interval. $T_a \in \mathbb{R}_{>0}$ is the time interval between two advertising events (in seconds), which is bounded by $T_l \leq T_a \leq T_u$, where $T_u = 10$ s and $T_l = 0.1$ s are, respectively, the upper and lower bounds of the advertising interval specified by the Bluetooth specification. $E_\sigma \in \mathbb{R}_{>0}$ is the energy consumption during the sensing task, $E_a \in \mathbb{R}_{>0}$ is the energy consumption during the advertisement event, and $P_i \in \mathbb{R}_{>0}$ is the power consumption during the idle state of the beacon. Parameters E_σ, E_a, P_i, and P_m are obtained empirically and may vary depending on the hardware and firmware specifications.

In order for the energy harvesting beacon to be self-sustainable, the energy harvested must be always greater than or equal to its consumption. Therefore, the minimum area of the solar panel, $A \in \mathbb{R}_{>0}$, to enable self-sustainability can be derived from the above constraint:

$$A \sum_{t=1}^{N} \frac{P_p(L(t))}{N} = P_b(T_a, T_\sigma)$$
$$\Rightarrow A = N \frac{P_b(T_a, T_\sigma)}{\sum_{t=1}^{N} P_p(L(t))} \tag{2}$$

where $\mathbb{R}_{\geq 0}$ is a set of nonnegative real numbers including all positive numbers and zero defined as $\mathbb{R}_{\geq 0} = \{x \in \mathbb{R} | x \geq 0\}$, $P_p(L(t)) \in \mathbb{R}_{\geq 0}$ is a power output density of a PV panel, $\mathbb{R}_{\geq 0}$ is a set of nonnegative real numbers including all positive numbers and zero defined as $\mathbb{R}_{\geq 0} = \{x \in \mathbb{R} | x \geq 0\}$, and $L(t) \in \mathbb{R}_{\geq 0}$ is a illuminance of the ambient light at timeslot $t \in \{1, 2, \ldots, N\}$, where each timeslot has a timeslot duration, T_L, of 1 h. The number of timeslots, N, is given by $mN^{\min}$ and bounded by $N^{\min} \leq N \leq N^{\max}$, where $N^{\min} \in \mathbb{N}$ is the number of timeslots in a single cycle of the illuminance data and $m \in \mathbb{N}$ is the number of cycles in the entire collected data of $L(t)$. Therefore, the number of cycles, m, is given by $m = \{1, 2, \ldots, N/N^{\min}\}$. N is lower bounded by the number of timeslots in a single cycle of the data, K, such that the collected data can describe at least one cycle of the illuminance behavior to identify power surplus and deficit. On the other hand, N is upper bounded by $N^{\max}$, as the bound will help to reduce the computation/optimization cost. In this article, we have used 30 days as the upper bound.

Now that we have determined the area of the solar panel, A, the net power harvested/consumed at timeslot t, $P_n(L(t)) \in \mathbb{R}$, is given by

$$P_n(L(t), T_a, T_\sigma) = AP_p(L(t)) - P_b(T_a, T_\sigma). \tag{3}$$

Since $P_n(L(t))$ represents the sum of the harvested power and consumed power, $P_n(L(t))$ is always less than the total harvested energy and upper bounded by it, i.e., $P_n(L(t)) < AP_p(L(t))$. Note that the power of the supercapacitor, $P_n(L(t))$, can be negative if the power consumption is larger than the power harvested. Therefore, when $P_n(L(t)) > 0$, the supercapacitor is being charged with the harvested ambient light energy, when $P_n(L(t)) < 0$, the power is drawn from the supercapacitor, and when $P_n(L(t)) = 0$, the supercapacitor is neither being charged nor discharged, as the amount of harvested energy perfectly meets the energy requirements.

Based on the total power harvested/consumed, $P_n(L(t))$, the minimum capacitance of a supercapacitor can be found by comparing the amount of energy that could be stored on a supercapacitor and the total amount of negative $P_n(L(t))$ during which the energy harvesting device cannot self-sustain with the ambient light energy and must rely on the stored energy. Based on this constraint, the minimum capacitance of a supercapacitor, $C \in \mathbb{R}_{\geq 0}$, is given by

$$CE_c = \begin{cases} \overline{E}_+, & \text{if } \overline{E}_+ \leq \overline{E}_- \\ \overline{E}_-, & \text{otherwise} \end{cases}$$
$$\Rightarrow C = \min\left(\frac{\overline{E}_+}{E_c}, \frac{\overline{E}_-}{E_c}\right) \tag{4}$$

where $E_c \in \mathbb{R}_{>0}$ is the energy density of a supercapacitor, $\overline{E}_+$ is the average energy that could be used to charge the supercapacitor, and $\overline{E}_-$ is the average energy that is required for self-sustainable operation when there is not enough ambient light energy to support its operation. An illustration of E_+ and E_- is shown in Fig. 6, which is derived based on net power formulation. It should be noted that the supercapacitor capacitance is chosen between E_+ and E_- depending on which is smaller. If $\overline{E}_+ < \overline{E}_-$, $\overline{E}_+$ is chosen since the average harvested energy will usually be less than $\overline{E}_-$, and therefore, the supercapacitor will not be fully utilized, and it is unnecessary to choose a larger capacitance. By adopting such a design philosophy, the manufacturing cost of the beacon can be minimized along with its format factor and weight.

To calculate the lifetime of an energy harvesting device powered by both supercapacitor and a backup battery, the supercapacitor voltage behavior must be simulated based on the given

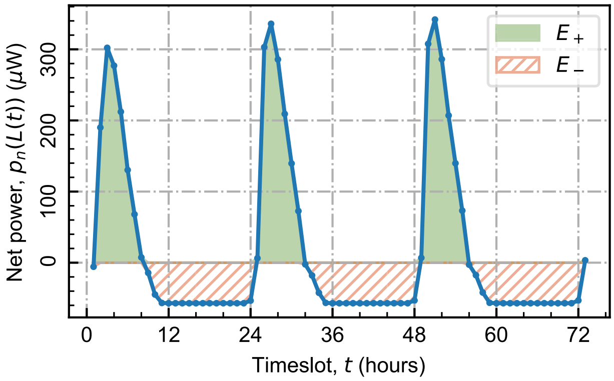

Fig. 6. Calculated net power of the energy harvesting device is plotted to show the harvestable amount of energy, E_+, and the required amount of energy in the absence of ambient light, E_-.

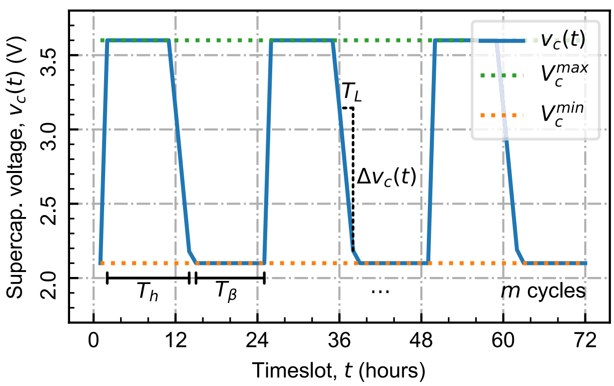

Fig. 7. Calculated voltage of the supercapacitor is plotted to show the time of operation supported by harvested energy, T_h, and the time of operation supported by a backup battery, T_β.

environmental data. With the simulated supercapacitor voltage, the time period being powered by the ambient light and by the backup battery can be identified. The supercapacitor voltage behavior is given by

$$V_c(t+1) = \begin{cases} V_c^{\max}, & \text{if } V_c(t) + \Delta V_c(t) \geq V_c^{\max} \\ V_c^{\min}, & \text{if } V_c(t) + \Delta V_c(t) \leq V_c^{\min} \\ V_c(t) + \Delta V_c(t), & \text{otherwise} \end{cases} \tag{5}$$

where $V_c(t+1)$ is the voltage of the supercapacitor at timeslot $t+1$, $V_c(t)$ is the voltage of the supercapacitor at timeslot t, $t \in \{1, 2, \ldots, N\}$ is a timeslot synchronized with that of the illuminance data, and $\Delta V_c(t) \in \mathbb{R}$ is the increment in supercapacitor voltage at timeslot t and is given by $\Delta V_c(t) = T_L \frac{P_n(L(t), T_a, T_\sigma)}{C V_c(t)}$. Note that the equation assumes that the initial supercapacitor voltage level is $V_c^{\min}$, i.e., $V_c(1) = V_c^{\min}$.

Based on the simulated supercapacitor voltage, the time duration powered by the backup battery, T_β, can be found as shown in Fig. 7, which is plotted based on previous supercapacitor voltage formulation. During T_β, the voltage of the supercapacitor, $V_c(t)$, is less than its minimum requirement, $V_c^{\min}$. Therefore, since the harvested and stored energy is depleted, a backup battery must be used to power the application. A portion of time-powered by

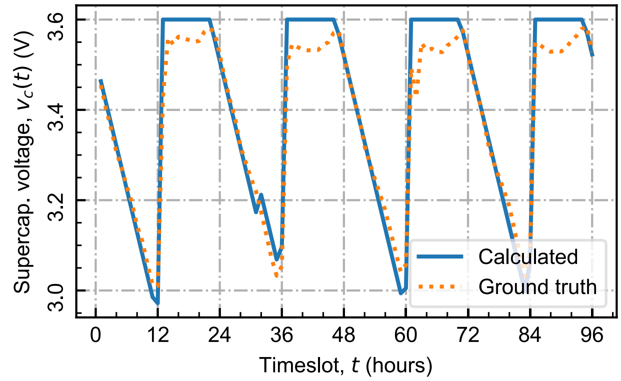

Fig. 8. Calculated voltage of the supercapacitor is plotted against a ground truth to demonstrate the accuracy of the proposed formulations.

TABLE IV
EXTENDED LIFETIME OF AN ENERGY HARVESTING SENSOR FOR VARYING CAPACITANCE OF SUPERCAPACITOR

Capacitance (F)	**Extended Lifetime** (years)
0.5	0.54 (+98%)
1.0	0.75 (+175%)
1.5	1.18 (+330%)
50	2.36 (+700%)

the backup battery, p_β is given by

$$p_\beta = \frac{\overline{T}_\beta}{T_L N^{\min}} \tag{6}$$

where $\overline{T}_\beta \in \mathbb{R}_{\geq 0}$ is the time duration powered by the backup battery, $N^{\min}$ is the number of timeslots in a single cycle, and T_L is the timeslot duration. Based on this insight of p_β, the extended lifetime, t_l, is given by

$$t_l = \frac{E_\beta}{p_\beta P_b(T_a, T_\sigma)} \tag{7}$$

where $E_\beta \in \mathbb{R}_{\geq 0}$ is an energy stored in a backup battery, and the denominator represents the reduced hybrid power consumption with the contributions from energy harvesting hardware. The proposed methodology and formulations are verified with real-life data collected in a greenhouse, as shown in Fig. 8. The extended lifetime of the energy harvesting device in comparison to that of the traditional battery-powered one is shown in Table IV. It shows that the different capacitance values can be chosen to support self-sustainable operation based on the power requirement of the sensing application.

V. FIELD-TEST RESULTS AND DISCUSSION

Based on the developed prototype of the luXSensing beacon, the following section details the field-test setup and results. We first present our deployment environment, namely the desert greenhouse in Qatar, and the deployment methodology and locations of four units of luXSensing beacon around the greenhouse. Our field-test experience also hints at the tedious nature of deployment and management of a battery-powered sensing system and also the benefits the proposed batteryless system can induce. Then, the data collected with the luXSensing beacons from the desert greenhouse are presented. The results unveil various insights related to the greenhouse environment and further highlight the importance of the dense deployment of a sensing system.

A. Design Considerations and Prototyping

Based on the previously presented luXSensing beacon architecture, its hardware specifications, namely supercapacitor capacity and PV panel area, are determined based on the provided illuminance data and other qualitative design considerations. Here, we showcase three scenarios where each scenario has a different design consideration. The implementation of the proposed design methodology can be found on our GitHub page.[1]

In the first design, we compute the PV panel size only with the assumed power consumption of the luXSensing beacon and the collected illuminance data. In other words, we are strictly following the data and power consumption to guide our design process. Here, we assume that the luXSensing beacon consumes 30 μA of current. The calculated PV panel size of the first design is 65 mm^2, and the supercapacitor capacitance is 0.74 F. Although the first design minimizes the PV panel size and may work perfectly for an identical environment, it is not robust to dynamic changes in the environment, namely weather, season, and deployment locations. In the second design, we preprocess the illuminance data such that it will have an average of 1000 lx during noon time. We tune the illuminance data down such that we can support various deployment locations, especially those overcast environments. In other words, the second design should be able to harvest enough energy even when it is not exposed to direct sunlight. The PV panel size was calculated to be 900 mm^2 and the supercapacitor capacitance is 1.11 F in the second design.

In the third design, we fine-tune the design with the objective of minimizing the form factor of the device while maximizing its sustainability. For the supercapacitor, we found that 1.0- and 1.5-F supercapacitors generally share the same packaging and, therefore, have the same form factor. Naturally, we chose the 1.5-F supercapacitor over the 1.0-F one for a higher chance of self-sustainability. For the PV panel, we found that our printed circuit board (PCB) could not be smaller than 50$\times$60 mm^2 if we wanted to host all the electronic components including the supercapacitor, backup battery, and RF antenna. That is, the form factor of the luXSensing beacon is lower-bounded by the size of the PCB. Therefore, the PV panel size can be increased to cover a similar area to improve the sustainability of the device while keeping its form factor more or less the same. Hence, we chose a PV panel with a size of 58$\times$65 mm^2. Based on these chosen components, the luXSensing beacons are prototyped as shown in Fig. 10.

We have also compared the performance of the optimized design of the luXSensing beacon with other energy harvesting beacon devices, as shown in Table V. Since existing energy harvesting beacons are equipped with different chipsets and sensors, it would not be fair to directly compare their sustainability and energy performance. Therefore, we have conducted numerical experiments only using their solar panel size and supercapacitor capacitance. Here, we assume that the beacons are consuming 30 μA of current and are equipped with 120-mAh backup batteries. The performance of the beacons is measured in terms of sustainable time and extended lifetime. Sustainable time refers to the average duration of time in a day during which the beacon was operating solely with the harvested energy. For example, 8.57 h of sustainable time reported for the GCell beacon indicates that the beacon was only able to operate, on average, 8.57 h out of 24 h with the harvested energy. In the remaining 15.43 h, it would not be able to operate unless it is equipped with a backup battery. On the other hand, extended lifetime simply refers to the battery lifetime that is now extended thanks to the use of energy harvesting hardware.

TABLE V
PERFORMANCE COMPARISONS BETWEEN THE PROPOSED LUXSENSING BEACON AND EXISTING ENERGY HARVESTING BEACONS WITH SENSORS

	Solar panel size (mm x mm)	Supercapacitor capacity (F)	Sustainable time (hours)	Extended Lifetime (years)
GCell [15]	20 × 70	0.002	8.57	0.71 (×1.56)
Cypress [13]	15 × 15	0.2	5.64	0.6 (×1.31)
TIDA [16]	58.42 × 58.42	0.008	9.5	0.76 (×1.66)
LuXSensing Beacon (ours)	58 × 65	1.5	23.14	12.79 (×28)

From Table V, we can see that the proposed luXSensing beacon can achieve a sustainable time of 23.14 h, while other beacons are achieving a maximum of 9.5 h. We are not achieving 24 h of sustainable time due to certain extreme weather conditions during which the supercapacitor may not get fully charged to support self-sustainable operation in the nighttime. The sustainable time can be translated to extended lifetime which amounts to around 13 years, which is $\times$28 extended compared to the original lifetime. Noting that the size of the luXSensing beacon device is similar to or even smaller than the GCell or TIDA beacon, the performance demonstrated by the proposed luXSensing beacon is even more impressive. The experimental result demonstrates the importance of choosing the proper hardware specifications for self-sustainable operation.

B. Deployment Environment and Setup

The prototype sensing system has been deployed in a self-sufficient greenhouse, named QTFA farm, which is located at (25°22′29.1″N, 51°14′37.7″E). Before prototyping and deploying the luXSensing beacons, we have collected the illuminance data at our deployment location over 40 days starting from early January to mid February. During our data collection period, we observed around 8 h of sunlight. Of course, there may be some performance deviation due to the changes in the environment over the year, namely the average length of day. However, we want to highlight that the proposed design methodology is generic to various scenarios because it is data driven. In other words, the performance variation due to change of season or location can be easily attenuated with collection of more environmental data and subsequent fine-tuning of the hardware

[1] https://github.com/sbeacon/luXSensing-Beacon

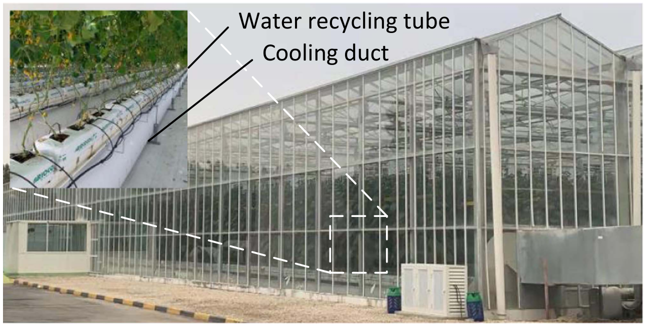

Fig. 9. Desert greenhouse located in Qatar (Al Shaniya Farm, 96FX+FWR, Ash-Shahaniyah).

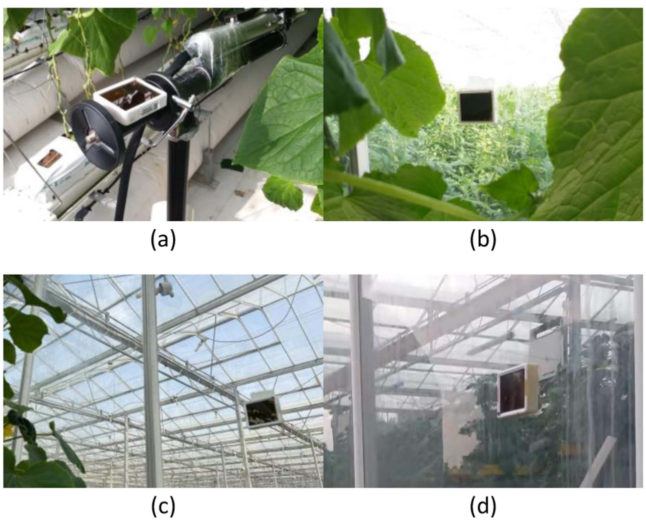

Fig. 10. Experimental setup of (a) Sen_1 at 1 m high without shade, (b) Sen_2 at 1 m high with shade, (c) Sen_3 at 3 m high without shade, and (d) Sen_4 at 3 m high outside the greenhouse.

specifications. The test site has a high annual temperature (mean monthly temperatures between 16 °C and 38 °C), extremely low rainfall (mean annual precipitation below 100 mm), and strong solar radiation (maximum 116 klx) [37]. The greenhouse has an area of 2500 m^2 and a height of 8 m with the exterior covered entirely in silica glass (see Fig. 9). Crops including cucumber and tomato are grown at the 1-m level, below which water recycling tubes and cooling ducts are installed. As demonstrated in Fig. 10, a total of four batteryless luXSensing beacons have been installed at different locations at the test site. They are, respectively, Sen_1 (at 1 m high inside the greenhouse without shade), Sen_2 (at 1 m high shaded by crops), Sen_3 (at 3 m high above crops), and Sen_4 (at 3 m high outside the greenhouse).

The system is proven to be able to work continuously for 24 h, as the supercapacitors can be fully charged during the daytime (6 A.M. to 5 P.M.) and supply energy to the beacons during the nighttime (5 P.M. to 6 A.M.). Fig. 11(a) (top) shows the three-point moving average of the four-week accumulated changes of the internal energy storage of the four luXSensing beacons. Fig. 11(b) shows the zoom-in measurements of day 4, while Fig. 11(c) shows those of day 25. As shown in the figure, during the daytime, the PV cells began to harvest energy at around 6 A.M., the time of sunrise, and restored energy storage of the beacons to 100%, sustaining their operation throughout the day. The time required for all luXSensing beacons to be fully charged was between 1.5 and 3 h. In particular, on day 25, although Sen_2 charged less quickly compared with the other sensors as it was shaded by crops and the amount of sunlight received was limited, the charging process could still be completed within just 3 h.

C. Results and Discussion

As the beacons were placed at different heights and locations, the measurement results verify their capability to capture microclimatic differences across the greenhouse. Fig. 11(a) (middle and bottom) shows that both the levels of illuminance and air temperature rose sharply at sunrise and reached a maximum approximately at noon before descending to a minimum at sunset. However, on a closer look at Fig. 11(b) and (c), the luXSensing beacons have captured the microclimatic differences in the greenhouse, which are demonstrated in both spatial and temporal terms.

Spatially speaking, the distributions of sunlight and heat vary according to the locational characteristics of where the beacons are placed. Take day 25 shown in Fig. 11(c) as an example. Sen_1 and Sen_4, which were placed in open areas, received more sunlight and, hence, recorded a higher level of illuminance when compared with Sen_2, which was shaded by plants. Similarly, among the four luXSensing beacons, Sen_2 recorded comparatively lower temperatures in the daytime due to the placement of cooling ducts below the crops as well as the shading effect of plants.

Temporally speaking, the trends of illuminance and air temperature readings change over time, reflecting changes in plant growth. In the initial stage of the crop growing cycle where the plant shading effect was not strong, readings of illuminance and air temperature recorded by the luXSensing beacons placed inside the greenhouse (Sen_1, Sen_2, and Sen_3) were close, as shown in Fig. 11(b). As time went by, Sen_2 and Sen_3 recorded increasingly lower levels of illuminance and air temperature, as shown in Fig. 11(c). This is due to the strengthening effect of plant shading as crops grew and their leaves covered larger areas, thus blocking more sunlight and reducing the air temperature.

These spatial and temporal differences observed in the readings taken by the four luXSensing beacons demonstrate the importance of a wide sensor grid to detect subtle environmental differences within the greenhouse. Compared with traditional greenhouse monitoring systems, which can only give an overall measurement of environmental conditions, the installation of a wide sensor grid is made possible by the batteryless luXSensing beacons due to their ease of deployment and cost-effectiveness. By providing a more comprehensive and detailed spatial and temporal observation of environmental conditions, the luXSensing beacons allow microclimate mapping of the greenhouse, which is particularly crucial to the feasibility of precision agriculture.

The energy headroom opens up the possibility for integrating more sensors (e.g., humidity and CO_2 concentration sensors) into the system to realize a more powerful sensor node, which

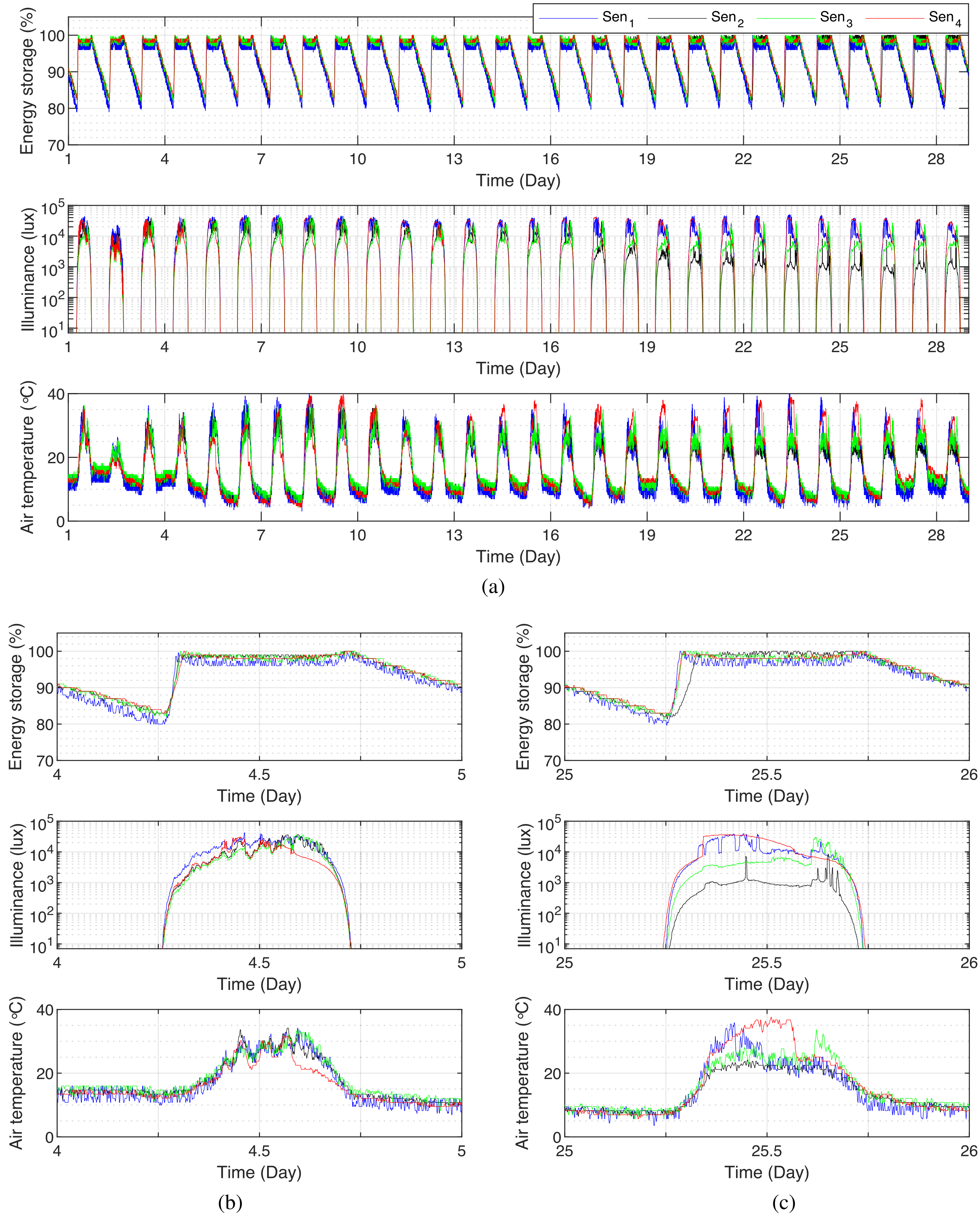

Fig. 11. Accumulated measurements of (a) (top) energy storage, (middle) illuminance, and (bottom) air temperature of the four luXSensing beacons for 28 days, (b) zoom-in measurements of day 4, and (c) zoom-in measurements of day 25.

is conducive to more thorough data collection and monitoring. Feedback from sensor readings to the control system can be utilized to achieve the homogenization of physical conditions and autonomous environmental control in greenhouses, for example, by regulating airflow in cooling ducts and manipulating rooftop shading systems.

The limitation of the proposed method, which is prevalent in all solar-cell-powered devices, is the dust that gradually deposits on the solar cell surface, which can degrade energy harvesting efficiency. To address this limitation, various hybrid energy harvesting methods integrating thermal or RF energy can be investigated in the greenhouse setting. The second limitation of this work is that our package design is still not 100% compatible with the plant support pole inside the greenhouse. Currently, our device can be handily deployed on the greenhouse glass wall. Different package designs that can hang on top of the plant should be investigated and developed in the future.

VI. Conclusion

This article presented: 1) a novel design methodology for energy harvesting devices; 2) a prototype of luXSensing beacon, a compact, cost-effective, and self-powered sensing system; and 3) field-test results of luXSensing beacon deployed for monitoring microclimatic conditions in greenhouses. Provided the illuminance data of the deployment environment, the proposed design methodology enabled quick and easy selection of component specifications, namely the PV panel's area, and the supercapacitor's capacitance. Such a design methodology is generic to all the energy harvesting devices and easily adaptable for different communication and harvesting technologies. Furthermore, we presented an extended lifetime formulation of a hybrid energy harvesting device equipped with a backup battery. Based on the proposed design methodology, a prototype of the luXSensing beacon was developed and the capability of the sensing system was verified via a deployment in a desert greenhouse in Qatar. As a proof of concept, the system achieved batteryless operation while continuously providing measurements of air temperature and illuminance at specific locations in a 24/7 manner. The proposed sensing system overcomes the limitations of bulkiness, high energy consumption, and high maintenance cost of conventional battery-powered sensors, enabling its large-scale deployment in greenhouses. The system is applicable and beneficial to the reduction of energy consumption and associated LCCs, maintenance of the homogeneity of the growing environment of crops, and the optimization of food production.

References

[1] A. F. Subahi and K. E. Bouazza, "An intelligent IoT-based system design for controlling and monitoring greenhouse temperature," *IEEE Access*, vol. 8, pp. 125488–125500, 2020.

[2] B. M. Huber, F. J. Louws, and R. Hernández, "Impact of different daily light integrals and carbon dioxide concentrations on the growth, morphology, and production efficiency of tomato seedlings," *Front. Plant Sci.*, vol. 12, 2021, Art. no. 615853.

[3] M. U. Sajid and Y. Bicer, "Comparative life cycle cost analysis of various solar energy-based integrated systems for self-sufficient greenhouses," *Sustain. Prod. Consumption*, vol. 27, pp. 141–156, 2021.

[4] X. Geng et al., "A mobile greenhouse environment monitoring system based on the Internet of Things," *IEEE Access*, vol. 7, pp. 135832–135844, 2019.

[5] A. Hussain, I. Choi, Y. H. Im, and H. Kim, "Optimal operation of greenhouses in microgrids perspective," *IEEE Trans. Smart Grid*, vol. 10, no. 3, pp. 3474–3485, May 2019.

[6] M. C. Bozchalui, C. A. Cañizares, and K. Bhattacharya, "Optimal energy management of greenhouses in smart grids," *IEEE Trans. Smart Grid*, vol. 6, no. 2, pp. 827–835, Mar. 2015.

[7] Q. O. Ogunlowo et al., "Analysis of heat and mass distribution in a single- and multi-span greenhouse microclimate," *Agriculture*, vol. 11, no. 9, 2021, Art. no. 891.

[8] "Blue-Tooth BLE Devices, Location & Tracking IoT Software Solution," BeaconTrax, Ajax, ON, Canada, 2022. Accessed: Feb. 1, 2023. [Online]. Available: https://www.beacontrax.com/

[9] "TRAX10157—Lorawan Temperature & Humidity Sensor—Lorawan," BeaconTrax, Ajax, ON, Canada, 2020. Accessed: Feb. 1, 2023. [Online]. Available: https://www.beacontrax.com/product/trax10157-lorawan-temperature-humidity-sensor/

[10] "Hyperscale IoT—Always-on Self-Powered Wireless Systems", Everactive, Santa Clara, CA, USA, 2022. Accessed: Feb. 1, 2023. [Online]. Available: https://everactive.com/

[11] "Energy Harvesting Sensors 101," Everactive, Santa Clara, CA, USA, 2022. Accessed: Feb. 1, 2023. [Online]. Available: https://everactive.com/whitepapers/energy-harvesting-sensors-101/

[12] "Semiconductor & System Solutions," Infineon Technol., Neubiberg, Germany. Accessed: Feb. 1, 2023. [Online]. Available: https://www.infineon.com/

[13] "DigChip Electronics Component Database—CYALKIT-E02," DigChip datasheet. Accessed: Feb. 1, 2023. [Online]. Available: https://www.digchip.com/datasheets/parts/datasheet/115/CYALKIT-E02-pdf.php

[14] S. S. Alrwashdeh and H. Ammari, "Life cycle cost analysis of two different refrigeration systems powered by solar energy," *Case Stud. Thermal Eng.*, vol. 16, 2019, Art. no. 100559.

[15] "World's First Indoor Solar Powered iBeacon," GCell, Newport, U.K. Accessed: Feb. 8, 2023. [Online]. Available: https://gcell.com/gcell-launches-worlds-first-indoor-solar-powered-ibeacon

[16] "TIDA—00100: Indoor Light Energy Harvesting Reference Design for BLE Beacon Subsystem," Texas Instrum., Dallas, TX, USA. Accessed: Feb. 8, 2023. [Online]. Available: https://training.ti.com/tida-00100-indoor-light-energy-harvesting-reference-design-ble-beacon-subsystem

[17] W.-C. Shih, P. H. Chou, and W.-T. Chen, "A batteryless beacon based on dual ISM-band RF harvesting with solar-biasing current," in *Proc. 4th Int. Workshop Energy Harvesting Energy-Neutral Sens. Syst.*, 2016, pp. 7–12.

[18] P. Mekikis, A. Antonopoulos, E. Kartsakli, L. Alonso, and C. Verikoukis, "Connectivity analysis in wireless-powered sensor networks with batteryless devices," in *Proc. IEEE Glob. Commun. Conf.*, 2016, pp. 1–6.

[19] J. Huang, Y. Meng, X. Gong, Y. Liu, and Q. Duan, "A novel deployment scheme for green Internet of Things," *IEEE Internet Things J.*, vol. 1, no. 2, pp. 196–205, Apr. 2014.

[20] A. Khanna and S. Kaur, "Evolution of Internet of Things (IoT) and its significant impact in the field of precision agriculture," *Comput. Electron. Agriculture*, vol. 157, pp. 218–231, 2019.

[21] T. Ojha, S. Misra, and N. S. Raghuwanshi, "Internet of Things for agricultural applications: The state of the art," *IEEE Internet Things J.*, vol. 8, no. 14, pp. 10973–10997, Jul. 2021.

[22] A. Gutierrez, A. Ansuategi, L. Susperregi, C. Tubío, I. Rankic, and L. Lenža, "A benchmarking of learning strategies for pest detection and identification on tomato plants for autonomous scouting robots using internal databases," *J. Sens.*, vol. 2019, pp. 1–15, 2019.

[23] K. Fue, W. Porter, E. Barnes, and G. Rains, "An extensive review of mobile agricultural robotics for field operations: Focus on cotton harvesting," *AgriEngineering*, vol. 2, no. 1, pp. 150–174, 2020.

[24] D. Brunelli, A. Albanese, D. d'Acunto, and M. Nardello, "Energy neutral machine learning based IoT device for pest detection in precision agriculture," *IEEE Internet Things Mag.*, vol. 2, no. 4, pp. 10–13, Dec. 2019.

[25] D. Vasisht et al., "FarmBeats: An IoT platform for data-driven agriculture," in *Proc. USENIX Symp. Netw. Syst. Des. Implementation*, 2017, pp. 515–529.

[26] S. K. Roy, S. Misra, N. S. Raghuwanshi, and S. K. Das, "AgriSens: IoT-based dynamic irrigation scheduling system for water management of irrigated crops," *IEEE Internet Things J.*, vol. 8, no. 6, pp. 5023–5030, Mar. 2021.

[27] Y. W. Lin, Y. B. Lin, and H. N. Hung, "CalibrationTalk: A farming sensor failure detection and calibration technique," *IEEE Internet Things J.*, vol. 8, no. 8, pp. 6893–6903, Apr. 2021.

[28] M. Muñoz, J. L. Guzmán, J. A. Sánchez-Molina, F. Rodríguez, M. Torres, and M. Berenguel, "A new IoT-based platform for greenhouse crop production," *IEEE Internet Things J.*, vol. 9, no. 9, pp. 6325–6334, May 2022.

[29] K. S. Yıldırım, H. Aantjes, P. Pawełczak, and A. Y. Majid, "On the synchronization of computational RFIDs," *IEEE Trans. Mobile Comput.*, vol. 18, no. 9, pp. 2147–2159, Sep. 2019.

[30] L. P. Fraile, S. Tsampas, G. Mylonas, and D. Amaxilatis, "A comparative study of LoRa and IEEE 802.15.4-based IoT deployments inside school buildings," *IEEE Access*, vol. 8, pp. 160957–160981, 2020.

[31] K. E. Jeon, J. She, P. Soonsawad, and P. C. Ng, "BLE beacons for Internet of Things applications: Survey, challenges, and opportunities," *IEEE Internet Things J.*, vol. 5, no. 2, pp. 811–828, Apr. 2018.

[32] I. Ghiat, F. Mahmood, R. Govindan, and T. Al-Ansari, "CO_2 utilisation in agricultural greenhouses: A novel 'plant to plant' approach driven by bioenergy with carbon capture systems within the energy, water and food nexus," *Energy Convers. Manage.*, vol. 228, 2021, Art. no. 113668.

[33] M. S. Farooq, S. Riaz, A. Abid, K. Abid, and M. A. Naeem, "A survey on the role of IoT in agriculture for the implementation of smart farming," *IEEE Access*, vol. 7, pp. 156237–156271, 2019.

[34] K. E. Jeon, J. She, J. Xue, S.-H. Kim, and S. Park, "luXbeacon—a batteryless beacon for green IoT: Design, modeling, and field tests," *IEEE Internet Things J.*, vol. 6, no. 3, pp. 5001–5012, Jun. 2019.

[35] C. Zhao et al., "Temperature increase reduces global yields of major crops in four independent estimates," *Nat. Acad. Sci.*, vol. 114, no. 35, pp. 9326–9331, 2017.

[36] T. N. Lin, B. Wang, and A. Bermak, "Review and analysis of instrumentation amplifier for IoT applications," in *Proc. IEEE 61st Int. Midwest Symp. Circuits Syst.*, 2018, pp. 258–261.

[37] D. Perez-Astudillo and D. Bachour, "Variability of measured global horizontal irradiation throughout Qatar," *Sol. Energy*, vol. 119, pp. 169–178, 2015.

[38] "Specification for Lithium Battery Model: CR2477, Power," Glory Battery Tech (HK) Co., Ltd., Hong Kong. [Online]. Available: http://www.farnell.com/datasheets/1496886.pdf

Kang Eun Jeon received the B.Eng. and Ph.D. degrees in electronic and computer engineering from the Hong Kong University of Science and Technology, Hong Kong, in 2015 and 2022, respectively.

He is currently a Postdoctoral Researcher with the Intelligent and Resource-Efficient Image Processing and Systems Design, Sungkyunkwan University, Suwon, South Korea. His research interests include on-device machine learning techniques that jointly optimize power consumption and model performance.

Tsz Ngai Lin received the B.Eng. degree in electronics and communications engineering from The University of Hong Kong, Hong Kong, in 2013, the M.Phil. degree in electronic and computer engineering from The Hong Kong University of Science and Technology, Hong Kong, in 2016, and the Ph.D. degree in computer science and engineering from Hamad Bin Khalifa University (HBKU), Doha, Qatar, in 2021.

During his academic journey, he contributed to research as a Research Associate with the Solid-State Sensing Laboratory, HBKU. He further expanded his expertise by serving as a Visiting Scholar with the University of Southampton, Southampton, U.K. He is currently a Senior Engineer with Qualcomm, Cambridge, U.K., where he continues to apply his knowledge and skills in the field. His research interests include precision analog and mixed-signal interface electronics, specializing in instrumentation amplifiers and low-power circuit designs.

James She received the Ph.D. degree in electrical and computer engineering from the University of Waterloo, Canada, in 2009. He is an Associate Professor with the Division of Information and Communication Technology, College of Science and Engineering, Hamad Bin Khalifa University, Doha, Qatar. His current research areas include Internet of Things and artificial intelligence technologies for sustainable, smart, and multimedia applications.

Dr. She is an Associate Editor for the IEEE TRANSACTIONS ON MULTIMEDIA and the *ACM Transactions on Multimedia Computing, Communications and Applications*.

Simon Wong received the B.Eng. degree in electronic engineering from the City University of Hong Kong, Hong Kong, and the M.Phil. degree in electronic and computer engineering from the Department of Electronic and Computer Engineering, Hong Kong University of Science and Technology, Hong Kong, in 2022.

He is currently with the Hong Kong University of Science and Technology. His research interests include secure and efficient social Bluetooth Low Energy beacon infrastructure for the Internet of Things applications.

Rajesh Govindan received the Ph.D. degree in environmental engineering from the Imperial College London, England, UK, in 2011.

He is currently with the College of Science and Engineering, Hamad Bin Khalifa University, Doha, Qatar. He has worked extensively on projects that involve the modeling of geospatial risks and uncertainties using multidisciplinary techniques from remote sensing and geographic information systems, geostatistics, and machine learning. Some of the key applications of his research include integrated development for predictive intelligence and optimization in food production systems in Qatar; technoeconomic analyses with the energy, water, and food nexus approach for resource allocation problems; and risk and uncertainty modeling and analyses for scenario development; and sustainability and resilience analyses, with special focus on energy, water, and food sectors in Qatar.

Tareq Al-Ansari received the B.Eng. degree in mechanical engineering from University College London, London. U.K., in 2008, the M.Phil. degree in engineering for sustainable development from the University of Cambridge, Cambridge, U.K., in 2011, and the Ph.D. degree in environmental engineering and sustainable development from Imperial College London, London, in 2016.

He is currently an Associate Professor and the Head of the Division of Sustainable Development, College of Science and Engineering, Hamad Bin Khalifa University, Doha, Qatar.

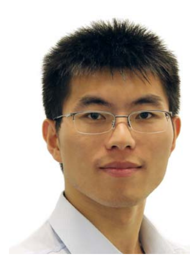

Bo Wang (Senior Member, IEEE) received the B.Eng. (Hons.) degree in electrical engineering from Zhejiang University, Hangzhou, China, in 2010, and the M.Phil. and Ph.D. degrees in electronic and computer engineering from the Hong Kong University of Science and Technology (HKUST), Hong Kong, in 2012 and 2015, respectively.

In 2015, he joined HKUST as a Postdoctoral Researcher and led the HKUST–Massachusetts Institute of Technology (MIT) Consortium project on wireless sensing node design for smart green building applications. In 2016, he was a Visiting Scientist with MIT, Cambridge, MA, USA. In 2017, he joined Hamad Bin Khalifa University, Al-Rayyan, Qatar, as a Founding Faculty, where he is currently an Associate Professor with the Division of Information and Computing Technology, College of Science and Engineering. His research interests include energy-efficient analog mixed-signal circuits, sensor and sensor interfaces, and heterogeneous integrated systems for in vitro/in vivo health monitoring.

Dr. Wang was a recipient of the IEEE ASP-DAC Best Design Award in 2016. He is a Technical Committee Member of the IEEE Circuits and Systems Society Committee on Sensory Systems. He is an Associate Editor for the IEEE SENSORS JOURNAL.